NANO · MICRO small
www.small-journal.com

Direct Observation of Vacancy-Cluster-Mediated Hydride Nucleation and the Anomalous Precipitation Memory Effect in Zirconium

*Si-Mian Liu, Shi-Hao Zhang, Shigenobu Ogata, Hui-Long Yang, Sho Kano, Hiroaki Abe, and Wei-Zhong Han**

Controlling the heterogeneous nucleation of new phases is of importance in tuning the microstructures and properties of materials. However, the role of vacancy—a popular defect in materials that is hard to be resolved under conventional electron microscopy—in the heterogeneous phase nucleation remains intriguing. Here, this work captures direct in situ experimental evidences that vacancy clusters promote the heterogeneous hydride nucleation and cause the anomalous precipitation memory effect in zirconium. Both interstitial and vacancy dislocation loops form after hydride dissolution. Interestingly, hydride reprecipitation only occurs on those vacancy loop decorated sites during cooling. Atomistic simulations reveal that hydrogen atoms are preferentially segregated at individual vacancy and vacancy clusters, which assist hydride nucleation, and stimulate the unusual memory effect during hydride reprecipitation. The finding breaks the traditional view on the sequence of heterogeneous nucleation sites and sheds light on the solid phase transformation related to vacancy-sensitive alloying elements.

1. Introduction

Solid phase transformation plays an important role in regulating microstructures, properties, and performances of materials.[1–3] Nucleation is usually the first step during phase transformation.[3] Most nucleation in solids as in liquids is heterogeneous, and relies on lattice defects, such as free surface, grain boundaries, interfaces, stacking faults, dislocations, and excess vacancies.[4–9] From the perspective of lowering the activation energy barrier, phase nucleation always occurs rapidly on the surface steps, and then on grain boundaries or interfaces. Stacking faults are less potent sites due to their lower energy in comparison to free surface and grain boundaries.[9] Dislocations assist phase nucleation by reducing the strain energy of phase embryo, supporting mass transport via pipe diffusion, or enhancing local solute segregation.[6–8] Notably, vacancies are least likely to serve as nucleation sites unless similar conditions for homogeneous nucleation are satisfied.[3] However, some indirect reports hint that excess vacancies may influence phase nucleation by increasing the diffusion rate of solute atoms or relieving misfit strain.[10,11] Since individual random vacancy is hardly to be distinguished by the resolution of a conventional electron microscope, especially during operando phase transformation, the role of vacancy and its clusters in phase nucleation and their precedence with other heterogeneous nucleation sites remains elusive.

Zirconium (Zr) alloys, as critical structural materials for fuel assemblies in nuclear reactors, are prone to hydrogen embrittlement as a result of formation of brittle hydrides.[12] Numerous brittle hydrides detract from the mechanical properties of Zr alloys and compromise the integrity of the cladding tubes.[13] The diversity of hydrides and the unique hybrid displacive-diffusive kinetics drastically increase the complexity of hydride phase transformation.[14–17] An anomalous memory effect is usually observed for the hydride precipitation, i.e., a hydride renucleates from the same position where the initial hydrides dissolve during thermal cycling.[18] The memory effect of hydride precipitation results in a greater extent of strain accumulation at the same location, which is the weakest point that accelerates cladding failure.[19] Postmortem experimental investigations and computer simulations have suggested that the tensile stress field around dislocations might assists hydride renucleation by accumulating hydrogen atoms.[20] However, the underlying

S.-M. Liu, W.-Z. Han
Center for Advancing Materials Performance from the Nanoscale
State Key Laboratory for Mechanical Behavior of Materials
Xi'an Jiaotong University
Xi'an 710049, China
E-mail: wzhanxjtu@mail.xjtu.edu.cn
S.-H. Zhang, S. Ogata
Department of Mechanical Science and Bioengineering
Osaka University
Osaka 560–8531, Japan
H.-L. Yang[+], S. Kano, H. Abe
Nuclear Professional School
The University of Tokyo
Tokai, Naka, Ibaraki 319–1188, Japan

The ORCID identification number(s) for the author(s) of this article can be found under https://doi.org/10.1002/smll.202300319

[+]Present address: School of Nuclear Science and Engineering, Shanghai Jiao Tong University, Shanghai 200240, China

DOI: 10.1002/smll.202300319

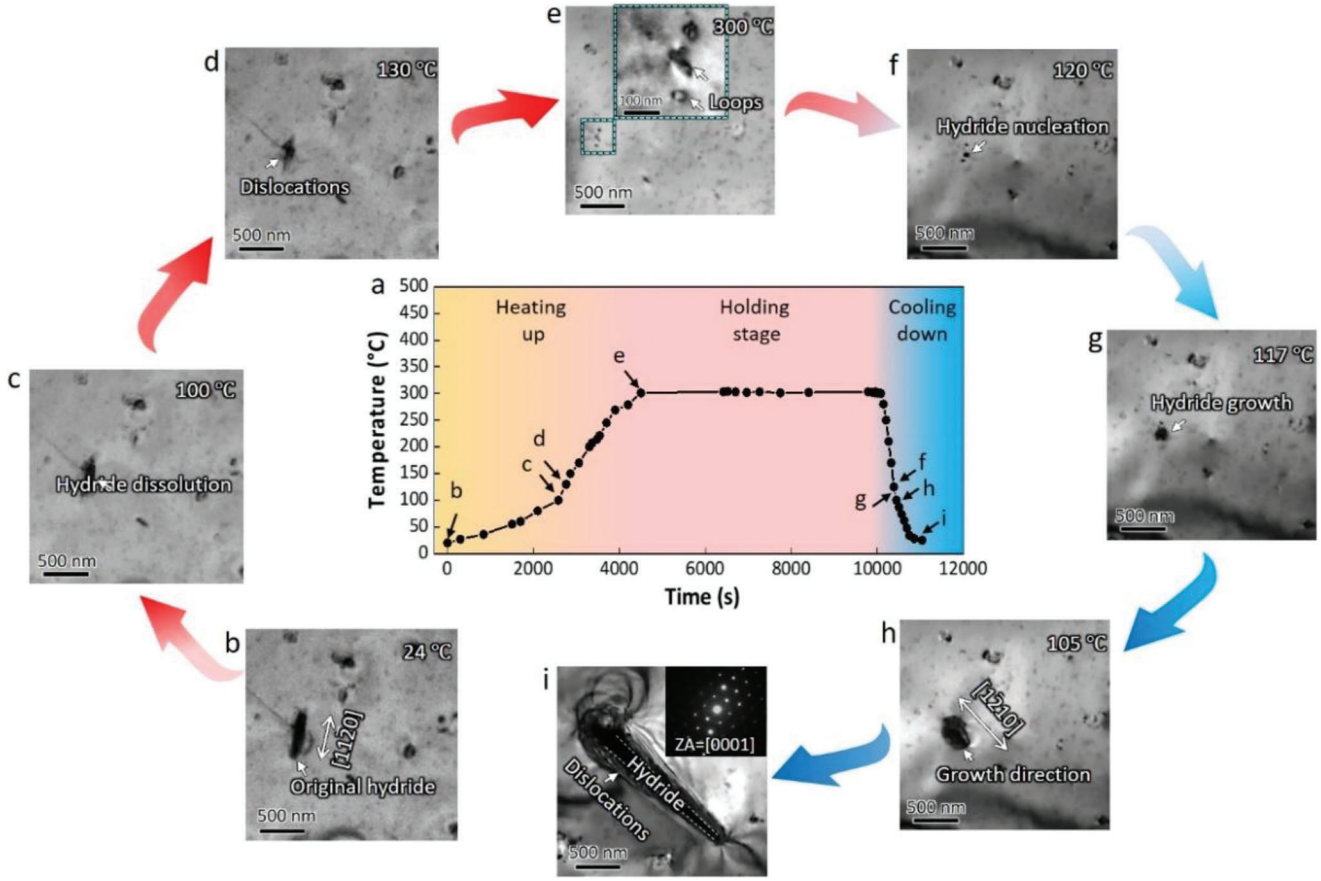

Figure 1. In situ observation of hydride dissolution and reprecipitation in Zircaloy-4. a) Variation of temperature with time during in situ thermal cycling. b–e) A hydride gradually dissolves when temperature increases from 24 °C to 300 °C. e) Enlarged transmission electron microscope (TEM) image highlights the dislocation loops. f) A new hydride starts to nucleate on the dislocation loops at $T = 120$ °C. g) The hydride grows rapidly within 1 s. h,i) The reprecipitated hydride grows along [1-2$\bar{2}$10] direction. See more details in Movie S1 (Supporting Information).

mechanism for the anomalous memory effect of hydride precipitation, likely relating to defect-stimulated heterogeneous phase nucleation, is indefinable due to the lack of intuitive experimental evidence.

Here, combining in situ heating transmission electron microscope (TEM) experiments and density functional theory (DFT) calculations, we report direct experimental evidence of hydride nucleation in Zr and elucidate the critical role of vacancy clusters in assisting hydride nucleation and causing the precipitation memory effect in Zr. Our finding highlights the important role of vacancy and their clusters in hydride precipitation and is beneficial for the design of high-performance nuclear energy structural materials.

2. Results

Recrystallized commercial Zircaloy-4 and pure Zr samples after hydrogen charging were used to investigate the hydride nucleation under one-time thermo-cycling in a TEM. The chemical compositions of the samples are shown in Table S1 (Supporting Information). After hydrogen charging, a large number of submicron-sized hydrides are formed and distributed uniformly within the grains (Figure S1, Supporting Information). During thermocycling, hydrides dissolve with increasing temperature and reprecipitate during cooling (**Figure 1**a). The detailed processes of the thermal cycling and the evolution of the hydrides are shown in Movie S1 (Supporting Information). Figure 1b shows an initial hydride with a size of 500 nm. As the temperature gradually increases to 100 °C, the hydride starts to dissolve, and shrink along [11$\bar{2}$0] (Figure 1c). With the temperature continues increasing, the hydride becomes thinner and thinner, leaving dislocation lines on both sides (Figure 1d). At 300 °C, the whole hydride dissolves, leaving some dislocation structures in the form of loops (Figure 1e). These dislocation loops remain stable even up to 400 °C. During the cooling stage with a rate of 0.5– 2 °C s^{-1}, a new hydride begins to nucleate from the dislocation loops (Figure 1f) at 120 °C. Just after 1 s, the hydride expands rapidly and grows along the [1$\bar{2}$10] direction (Figure 1g,h). The hydride lies on the basal plane and has a final length of 2 μm (Figure 1i), which is surrounded by a high density of dislocations. The reprecipitated δ-hydride has a face-centered cubic structure according to the diffraction pattern in Figure 1i. The orientation relationship between the new hydride and the matrix is $(111)_\delta$// $(0001)_{\alpha\text{-Zr}}$ and $[110]_\delta$// $[1\bar{2}10]_{\alpha\text{-Zr}}$.[17] The reprecipitated hydride alters the growth direction from [11$\bar{2}$0] to [1$\bar{2}$10].

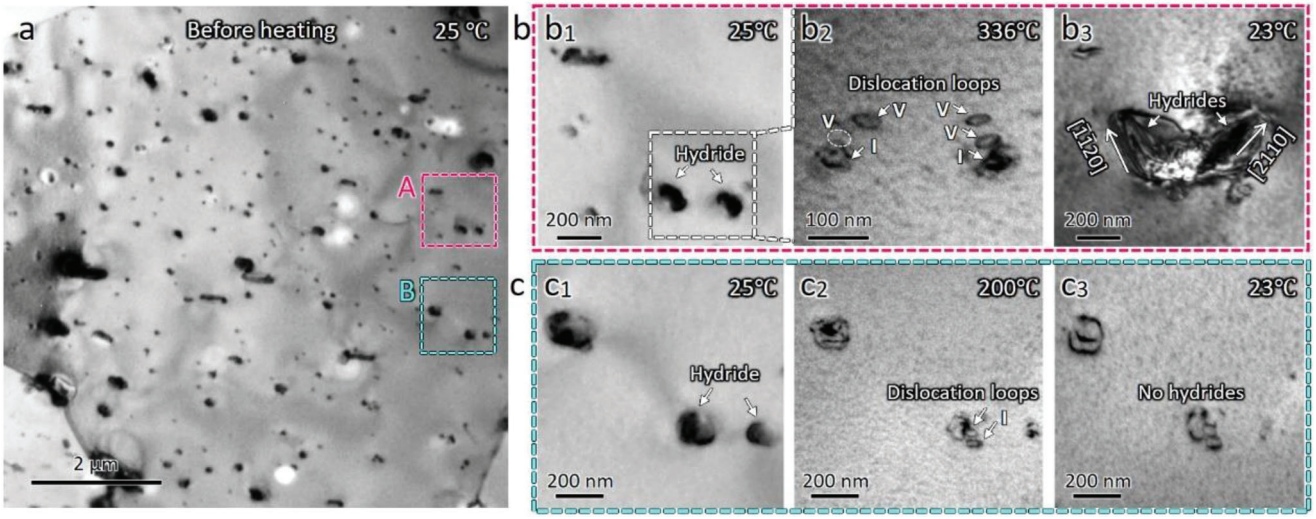

Figure 2. Heterogeneous hydride nucleation in Zircaloy-4 alloy. a) Small hydrides formed in the grain interior. b) Dissolution and reprecipitation of hydrides at vacancy dislocation loops. c) Hydride dissolution produces interstitial dislocation loops.

The dislocation structures formed after hydride dissolution were characterized in situ at high temperatures. **Figure 2**a shows the microstructures of some hydrides in a grain before heating. Regions A and B in Figure 2b were selected for detailed dynamic characterizations. In region A, two small hydrides become smaller in size as the temperature increases. The hydrides dissolve completely at 336 °C, and leave several nanosized dislocation loops, which include four vacancy loops and two interstitial loops (Figure 2b$_2$). When cooling down to room temperature, two hydrides renucleate and precipitate on the vacancy dislocation loops (Figure 2b$_3$). A similar analysis was also performed on region B. Two small hydrides with black contrast in Figure 2c$_1$ gradually dissolve and form two separate dislocation loops at 336 °C. These loops are interstitial in nature (Figure 2c$_2$), which are confirmed by the inside and outside contrast analysis during the temperature-holding stage.[21] With the temperature decrease to 23 °C, no hydrides reprecipitate at this location, as shown in Figure 2c$_3$. The detailed characterizations are shown in Figure S2 (Supporting Information) and Table S2 (Supporting Information).

More experiments were performed to clarify the competition of dislocation loops and dislocation lines on the hydride nucleation in Zircaloy-4 (**Figure 3**). All hydrides dissolve at 350 °C and produce both dislocation lines and dislocation loops at the region (Figure 3b). Different two-beam images of the dislocation loops at region C are obtained at 350 °C. Notably, a vacancy dislocation loop and an interstitial dislocation loop are identified in this region (Figure 3c). During the cooling, a new hydride nucleates at the vacancy dislocation loop and grows along the [$\bar{1}2\bar{1}0$] direction. While the interstitial dislocation loop and dislocation lines are retained in the matrix and no hydride is found to nucleate on these defects. After cooling down to room temperature, the

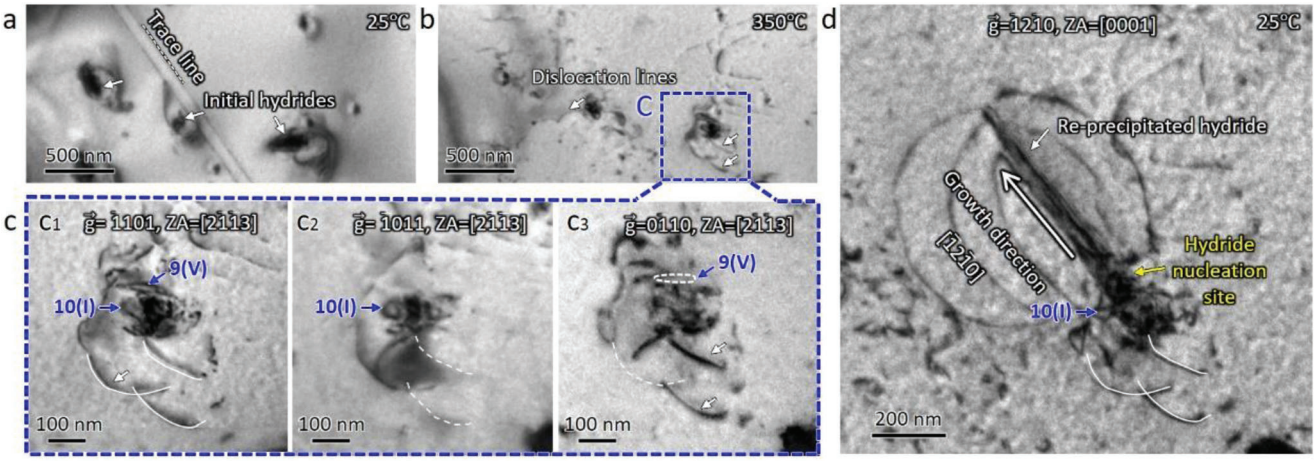

Figure 3. Characteristics of dislocation loops with hydride reprecipitation in Zircaloy-4 alloy. a) Hydrides before heating. b) Dislocation structures produced after hydrides dissolution. c) Different two-beam images showing the characteristics of dislocation loops in (b). d) Hydride nucleates on the vacancy dislocation loops.

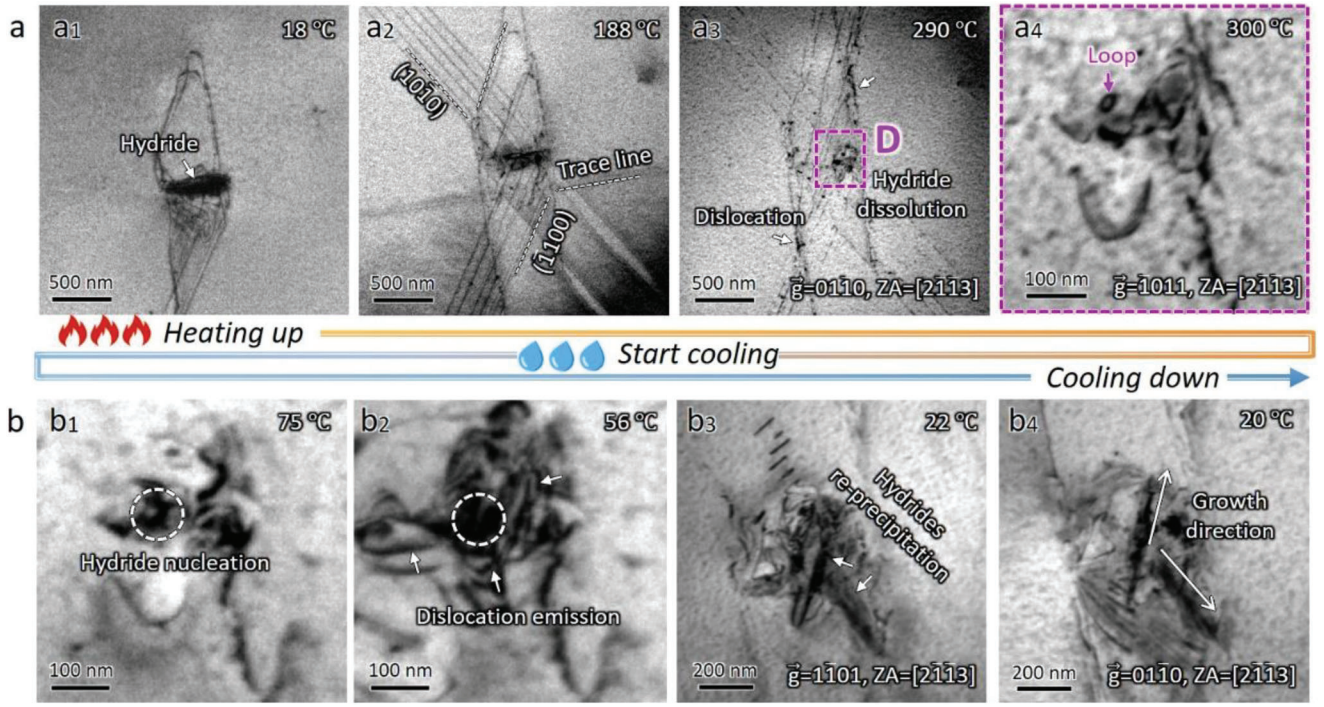

Figure 4. Hydride dissolution and reprecipitation in pure Zr. a) Dissolution of a hydride with temperature increasing from 18 °C to 300 °C. b) Two hydrides gradually nucleate and grow at the dislocation loops during cooling. See Movie S2 for more details.

reprecipitated hydride is surrounded by a butterfly-liked dislocation structure (Figure 3d).

The above experiments show that the character of dislocation loops has a marked effect on the reprecipitation of hydrides in Zircaloy-4. To exclude the influence of alloying elements, a pure Zr sample with similar hydrogen concentration was also examined (**Figure 4**). With the temperature increasing from 18 °C to 300 °C, a pre-existing hydride disappears gradually, and accompanies with the gliding of prismatic dislocations (Figure 4a). Both small dislocation loops and dislocation lines are produced after hydride dissolution (Figure 4a$_4$). The purple arrow indicates a vacancy dislocation loop (see details in Figure S3, Supporting Information). As the temperature dropped from 300 °C to 75 °C, the contrast of the dislocation loop changed significantly (Figure 4b$_1$). The hydride nucleates just on the vacancy dislocation loop. At 56 °C, the hydrides reprecipitates and grows up rapidly (Figure 4b), accompanied by emitting an array of $\frac{1}{3}\left[2\bar{1}\bar{1}0\right]$ dislocations (Movie S2, Supporting Information). This observation clarifies that the alloy elements play a negligible role during hydride precipitation. Notably, hydride nucleation rarely occurs at the interstitial dislocation loops in both the pure Zr and the Zircaloy-4 (Figure S4, Supporting Information and Table S2, Supporting Information).

3. Discussion

3.1. Origin of Dislocation Loops During Hydride Dissolution

After hydride dissolution, some interstitial or vacancy dislocation loops are visible at the location of the original hydride (see Figures 1–4). There are several possible ways to introduce dislocation loops.[22–24] First, electron beam irradiation could introduce point defects in metals. However, owing to a relatively high atomic displacement energy of 40 keV,[23] these dislocation loops are unlikely caused by the electron beam irradiation in Zr. Second, dislocation interactions with impenetrable hydrides could introduce dislocation loops via Orowan looping or Hirsch looping mechanisms.[24] The formation of dislocation loops accompanies with the dissolution of hydrides during the heating process (Figure 1). Hydrides dissolution is expected to relieve the tensile stress in the matrix and introduce a 17.2% volume variation with increasing temperature.[15,16] Local volume variation would introduce plastic deformation or numerous point defects in the surrounding matrix. As a consequence, hydride dissolution follows dislocation movement (see Movies S1 and S2, Supporting Information). However, there is no direct interaction between dislocations and hydrides during hydride dissolution.

Notably, with hydride dissolution, numerous vacancies or self-interstitials atoms are produced to accommodate the significant volume collapse, which can further evolve into vacancy or interstitial dislocation loops. Figure S5 (Supporting Information) shows the combination of vacancies and interstitial atoms with and without hydrogen atoms by DFT calculations. When hydrogen atoms are absent, vacancies and interstitial atoms gradually recombined with each other over time (Figure S5a, Supporting Information). Conversely, subsistent hydrogen atoms tend to bind with vacancies to form a hydrogenated vacancy dislocation loop as an embryo for later hydride reprecipitation.[25,26] The formed stable hydrogen-vacancy complexes could prevent the recombination of vacancies with interstitial atoms,[27] as shown by Figure S5b (Supporting Information). Therefore, the formation of dislocation loops is a result of hydride dissolution-induced

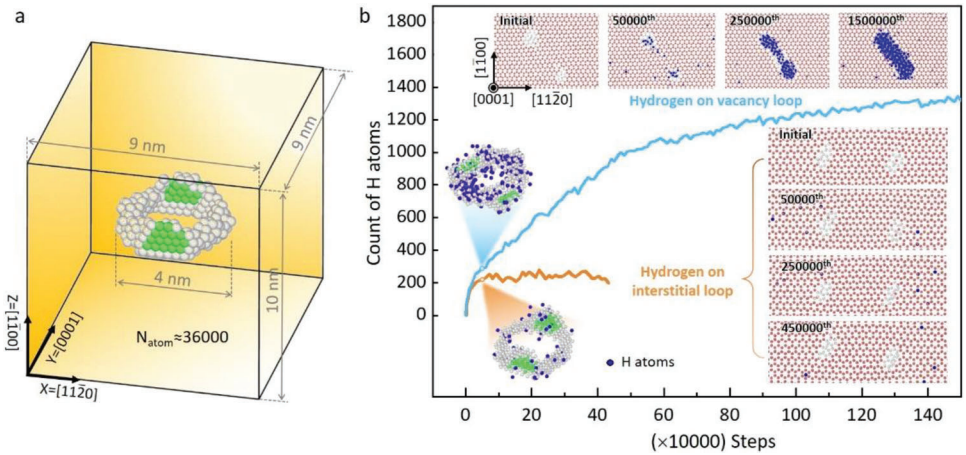

Figure 5. Segregation of hydrogen atoms at dislocation loops on prismatic plane. a) Atomic model of a prismatic dislocation loop in Zr. b) The number of hydrogen atoms segregation in the Zr models consisting of vacancy and interstitial dislocation loops on the prismatic plane. Inserts are cross-section snapshots of hydrogen atoms segregated at interstitial loops and vacancy loops. Atoms are colored according to the common neighbor analysis. Similar effects were observed for the dislocation loops on basal plane (see Figure S9).

local volume shrinkage and stabilizing of vacancies by hydrogen atoms.

3.2. Nucleation at Hydrogenated Vacancy Clusters

To reveal the underlying atomistic mechanism, density functional theory calculation and hybrid molecular dynamics (MD)/grand canonical Monte Carlo (GCMC) simulations were conducted to investigate the segregation of hydrogen atoms at vacancy and self-interstitial and their clusters. Figure S6a (Supporting Information) shows the atomic structures around a self-interstitial atom and a single vacancy in Zr. All possible configurations with different numbers of hydrogen atoms trapped at these sites around single vacancy and self-interstitial atom were relaxed via molecular statics (MS) simulation with both embedded atom method (EAM) potential and DFT calculations. The segregation energy difference for hydrogen atoms segregating from bulk to vacancy or self-interstitial atom is shown in Figure S7 (Supporting Information). The energy difference for a vacancy is much smaller than that to interstitial atom sites, indicating that hydrogen atoms tend to segregate near vacancy instead of interstitial. Moreover, up to 11 hydrogen atoms can be trapped in a single vacancy as a result of the lowest energy differences. Similar results were observed for hydrogen atom interactions with vacancies, divacancies and vacancies clusters.[28,29]

Figure 5 shows the hexagonal-shaped dislocation loops with Burgers vector $\frac{1}{3}\langle\bar{1}\bar{1}20\rangle$ in Zr. Both vacancy and interstitial-type dislocation loops are introduced by removing or adding a platelet of vacancies or interstitial atoms into the Zr matrix. The hydrogen chemical potentials (μ) in the hybrid MD/GCMC simulation were set to −2.90, −2.85, −2.80, and −2.75 eV, for which the equilibrium hydrogen concentrations in Zr bulk are 0.2, 2, 10, and 70 wppm, respectively. Figure 5b shows the number of hydrogen atoms segregated on the vacancy and interstitial dislocation loops in a Zr model with a hydrogen concentration of 70 wppm. About 1300 hydrogen atoms are segregated on a 4 nm-sized vacancy loop until hydrogen saturation, which is seven times more than that on the interstitial loop. Such an amount of hydrogen is sufficient to support hydride reprecipitation on the vacancy loop. Over GCMC simulation steps, more and more hydrogen atoms are trapped by the vacancy dislocation loops rather than the interstitial dislocation loops (Figure 5b, Movies S3 and S4, Supporting Information). This explains why the size of reprecipitated hydrides is much larger than the initial ones (see Figures 1–4). A similar trend is observed for the hydrogen concentrations in Zr bulk as well (Figure S8, Supporting Information).

Hydrogen atoms segregating at interstitial and vacancy dislocation loops on the basal plane is also calculated in the same way. Figure S9 (Supporting Information) shows both the intrinsic and extrinsic vacancy loops on the basal plane have a stronger attraction to hydrogen atoms than the interstitial loops, and are consistent with experiments.[30] In brief, both multiple vacancies and vacancy cluster evolved dislocation loops have a strong segregation effect on hydrogen atoms. Thus, a strong segregation ability of hydrogen atoms to vacancy clusters assists hydride nucleation on the vacancy-loop-decorated sites instead of interstitial ones. In addition, hydrostatic stress distribution around interstitial and vacancy loops with and without hydrogen atoms on both prismatic and basal planes are evaluated (see Figure S10, Supporting Information). A dilatational strain by stretching the lattice results in a strong tensile stress field inside the vacancy loops without hydrogen atoms near the loop edge. Inversely, one extra layer of atoms causes the compressive stress field in the interior of the interstitial loops, which is consistent with previous results.[31] The presence of hydrogen atoms neutralizes the stress field around the vacancy loops, as displayed in Figure S10 (Supporting Information). These unique local stress fields assist the preferential segregation of hydrogen.

3.3. New Order of Heterogeneous Nucleation Sites

Finally, we performed statistics of hydride nucleation and precipitation across several grains (Figure S11, Supporting Information). Before thermal cycling, hydrides are distributed

uniformly because the recrystallized grains are almost defect-free when hydrogen charging at 400 °C. Upon hydride dissolution, many dislocation lines and both interstitial/vacancy dislocation loops form due to volume collapse. Figure S11a (Supporting Information) shows that no hydride nucleates on dislocations, whereas hydrides only form on those vacancy loops in the interior of the grain (Figure S11b, Supporting Information) or adjacent to a grain boundary (Figure S11a_2, Supporting Information). Such an interesting phenomenon contradicts the conventional wisdom of heterogeneous nucleation site sequence.[3–11] Surfaces or grain boundaries are known to be the most favorable nucleation sites in heterogeneous phase nucleation, followed by dislocations and vacancy clusters.[3] Although hydrides are also frequently observed at grain boundaries or near the dislocation lines.[28,32] However, our in situ heating experiments confirm that vacancy clusters have a higher priority in hydride nucleation than grain boundaries and dislocation lines. Under a low level of hydrogen, the preferred segregation of hydrogen atoms at vacancy loops enhances the local concentration of hydrogen, and promotes the heterogeneous reprecipitation of hydrides (Figure S11a_3,b_3,c_3, Supporting Information). The observations well explain the anomalous memory effect associated with hydride reprecipitation.[18] Because of the strong binding of vacancies and their clusters with hydrogen atoms, they serve as preferential nucleation sites for hydrides. Such a mechanism also works for other alloys containing elements that have high binding energy with vacancies and serve as likely nucleation embryos in heterogeneous solid phase transformation.[33,34]

4. Conclusion

Our results provide direct experimental evidences of vacancy clusters-assisted hydride nucleation and reprecipitation in Zr. In situ heating experiments inside a TEM combined with dynamic dislocation loop characterizations and atomistic simulations reveal that the vacancy dislocation loops act as preferential nucleation sites to facilitate the precipitation of hydrides, providing a reasonable explanation for the frequently observed anomalous memory effect during hydride reprecipitation. Preferential segregation of hydrogen atoms at vacancies and the tensile stress field around vacancy-type defects are the origins of vacancy clusters as favored hydride nucleation sites over dislocations and grain boundaries. The present finding sheds light on the solid phase transitions related to vacancy-sensitive alloying elements.

Supporting Information

Supporting Information is available from the Wiley Online Library or from the author.

Acknowledgements

This research was supported by the National Natural Science Foundation of China (Grant Nos. 52301019, 51922082 and 51971170) and the 111 Project of China 2.0 (Grant No. BP0618008). S.M.L. acknowledges the financial support from the Postdoctoral Innovation Talents Support Program (BX20220245) and the China Scholarship Council (CSC). S.H.Z. and S.O. were supported by the JSPS Postdoctoral Fellowships for Research in Japan (Sstandard), the Grant-in-Aid for JSPS Research Fellow (Grant Number 22F22056) and the JSPS KAKENHI (Grant No. JP22KF-241), and were used computational resources of supercomputer Fugaku provided by the RIKEN Center for Computational Science (Project IDs: hp230205 and hp 230212), the large-scale computer systems at the Cybermedia Center, Osaka University, and the Large-scale parallel computing server at the Center for Computational Materials Science, Institute for Materials Research, Tohoku University. S.O. acknowledges the support by the Ministry of Education, Culture, Sport, Science and Technology of Japan (Grant No. JPMXP1122684766), Promoting Researches on the Supercomputer Fugaku, Computational Research on Materials with Better Functions and Durability Toward Sustainable Development (Grand No. JPMXP1020230325), and Data-Driven Research Methods Development and Materials Innovation Led by Computational Materials Science (Grant No. JPMXP1020230327), and the support by JSPS KAKENHI (Grant Nos. JP21K18675, JP18H05453, JP17H01238, and JP17K18827). The experiments were carried out under the collaborative research project at the Nuclear Professional School, School of Engineering, The University of Tokyo. A part of this work was supported by the MEXT Innovative Nuclear Research and Development Program (Grant No. JPMXD0220354500).

Conflict of Interest

The authors declare no conflict of interest.

Author Contributions

S.M.L. conducted the in situ experiments under the guidance of W.Z.H. and H.A. S.H.Z. and S.O. performed the density functional theorycalculations and the grand canonical Monte Carlo simulations. H.L.Y. assisted the in situ TEM thermal cycling operation. S.M.L. and W.Z.H. wrote the paper with input from other coauthors. All authors discussed and analyzed the results and contributed to the theoretical analysis.

Data Availability Statement

The data that support the findings of this study are available from the corresponding author upon reasonable request.

Keywords

dislocation, hydride, nucleation, vacancy, zirconium

Received: January 11, 2023
Revised: August 20, 2023
Published online:

[1] H. L. Huang, Y. Wu, J. Y. He, H. Wang, X. J. Liu, K. An, W. Wu, Z. P. Lu, *Adv. Mater.* **2017**, *29*, 1701678.
[2] X. Q. Fu, X. D. Wang, B. K. Zhao, Q. H. Zhang, S. Y. Sun, J. J. Wang, W. Zhang, L. Gu, Y. S. Zhang, W. Z. Zhang, W. Wen, Z. Zhang, L. Q. Chen, Q. Yu, E. Ma, *Nat. Mater.* **2022**, *21*, 290.
[3] D. A. Porter, K. E. Easterling, M. Sherif, *Phase Transformation in Metals and Alloys*, CRC Press, New York **2009**.
[4] J. Yan, A. M. Hodge, *J. Alloys Compd.* **2017**, *703*, 242.
[5] Y. Chen, X. Y. Fang, Y. Brechet, C. R. Hutchinson, *Acta Mater.* **2014**, *81*, 291.
[6] S. Y. Hu, L. Q. Chen, *Acta Mater.* **2001**, *49*, 463.
[7] W. A. Cassada, G. J. Shiflet, W. A. Jesser, *Acta Metall. Mater.* **1992**, *40*, 2101.

[8] Y. Song, T. N. Baker, *Mater. Sci. Technol.* **2013**, *10*, 406.
[9] J. M. Silcock, W. J. Tunstall, *Philos. Mag.* **1964**, *10*, 361.
[10] A. Picasso, A. Somoza, A. Tolley, *J. Alloys Compd.* **2009**, *479*, 129.
[11] S. H. Kim, S. J. Kang, M. H. Park, C. W. Yang, H. C. Lee, H. N. Han, M. Kim, *Acta Mater.* **2015**, *83*, 499.
[12] Y. J. Jia, W. Z. Han, *Materials* **2023**, *16*, 2419.
[13] A. Zielinski, S. Sobieszczyk, *Int. J. Hydrogen Energy* **2011**, *36*, 8619.
[14] J. H. Root, W. M. Small, D. Khatamian, O. T. Woo, *Acta Mater.* **2003**, *51*, 2041.
[15] O. Zanellato, M. Preuss, J. Y. Buffiere, F. Ribeiro, A. Steuwer, *J. Nucl. Mater.* **2012**, *420*, 537.
[16] Y. J. Jia, I. J. Beyerlein, W. Z. Han, *Acta Mater.* **2021**, *216*, 117146.
[17] S. M. Liu, A. Ishii, S. B. Mi, S. Ogata, J. Li, W. Z. Han, *Small* **2022**, *18*, 2105881.
[18] G. J. C. Carpenter, J. F. Watters, *J. Nucl. Mater.* **1978**, *26*, 1225.
[19] A. Hermann, S. K. Yagnik, D. Gavillet, in *15th International Symposium on Zirconium in the Nuclear Industry*, ASTM, Sunriver, OR **2009**.
[20] G. P. M. Leyson, B. Grabowski, J. Neugebauer, *Acta Mater.* **2015**, *89*, 50.
[21] S. M. Liu, W. Z. Han, *Tungsten* **2021**, *3*, 470.
[22] T. Diaz de la Rubia, M. W. Guinan, *Phys. Rev. Lett.* **1991**, *66*, 2766.
[23] R. F. Egerton, R. Mcleod, F. Wang, M. Malac, *Ultramicroscopy* **2010**, *110*, 991.
[24] S. Xu, D. L. McDowell, I. J. Beyerlein, *Acta Mater.* **2019**, *174*, 160.
[25] C. I. Maxwell, E. Torres, J. Pencer, *J. Nucl. Mater.* **2018**, *511*, 341.
[26] M. Christensen, W. Wolf, C. Freeman, E. Wimmer, R. B. Adamson, L. Hallstadius, P. E. Cantonwine, E. V. Mader, *J. Phys.: Condens. Matter* **2015**, *27*, 025402.
[27] P. J. Yang, Q. J. Li, T. Tsuru, S. Ogata, J. W. Zhang, H. W. Sheng, Z. W. Shan, G. Sha, W. Z. Han, J. Li, E. Ma, *Acta Mater.* **2019**, *168*, 331.
[28] N. A. P. Kiran Kumar, J. A. Szpunar, Z. He, *J. Nucl. Mater.* **2010**, *403*, 101.
[29] S. M. Liu, I. J. Beyerlein, W. Z. Han, *Nat. Commun.* **2020**, *11*, 5766.
[30] C. Varvenne, O. Mackain, L. Proville, E. Clouet, *Acta Mater.* **2016**, *102*, 56.
[31] C. Dai, P. Saidi, Z. Yao, M. R. Daymond, *Acta Mater.* **2017**, *140*, 56.
[32] V. S. Arunachalam, B. Lehtinen, G. Östberg, *J. Nucl. Mater.* **1967**, *21*, 241.
[33] A. Bakaev, D. Terentyev, X. He, E. E. Zhurkin, D. Van Neck, *J. Nucl. Mater.* **2014**, *451*, 82.
[34] D. Shin, C. Wolverton, *Acta Mater.* **2010**, *58*, 531.